

# Generation of the $(3/2)\omega_0$ harmonic of the neodymium-laser radiation during the heating of spherical targets

A. I. Avrov, V. Yu. Bychenkov, O. N. Krokhin, V. V. Pustovalov, A. A. Rupasov, V. P. Silin, G. V. Sklizkov, V. T. Tikhonchuk, and A. S. Shikanov

*P. N. Lebedev Physics Institute, USSR Academy of Sciences*  
(Submitted July 30, 1976)  
*Zh. Eksp. Teor. Fiz.* 72, 970-982 (March 1977)

The spectral composition and intensity of the  $(3/2)\omega_0$  harmonic generated during the heating of glass microspheres by the radiation of a "Kalmar" high-power neodymium laser have been measured. The phenomenon is interpreted with the aid of the theory of parametric turbulence, and the possibility of determining the parameters of the laser plasma in the region of a quarter of the critical density on the basis of the spectral measurements on the  $(3/2)\omega_0$  harmonic is demonstrated.

PACS numbers: 42.65.Cq, 52.50.Jm

## INTRODUCTION

Within the framework of the presently soluble problem of laser thermonuclear fusion,<sup>[1]</sup> the study of the energy and spectral characteristics of the radiation scattered by the laser plasma at the fundamental frequency, as well as at the harmonic frequencies, of the heating radiation is of interest. The spectral analysis of the radiation generated by the plasma is an effective method of laser-plasma diagnostics. Such investigations allow us, on the one hand, to determine a number of dense-plasma parameters—the electron-density gradient in the vicinity of the region of the critical density,<sup>[2]</sup> the electron temperature in this region<sup>[3]</sup>—and, on the other, to draw conclusions about the heating efficiency and the mechanisms underlying the absorption of laser radiation by a plasma.<sup>[2,4-6]</sup> The distinctive features of the generation of the second harmonic  $2\omega_0$  have been studied in adequate detail (see, for example, the review article<sup>[7]</sup>). Results have been published of experiments in which the  $\frac{3}{2}\omega_0$  harmonic was investigated<sup>[8-11]</sup> for the case of sharp focusing of the heating radiation on the target.

In the present paper we investigate the generation by a laser plasma of the  $\frac{3}{2}\omega_0$  harmonic of the heating radiation for the case of spherical heating of hollow  $\text{SiO}_2$ -glass microspheres. A detailed analysis is carried out of the spectral composition of the radiation emitted from the plasma at frequencies close to  $\frac{3}{2}\omega_0$ . The principal nonlinear mechanisms determining the intensity and spectrum of the radiation of frequency  $\frac{3}{2}\omega_0$  generated by the plasma are discovered. On the basis of a comparison of the results of the theory with experiment we propose a method for determining the plasma parameters in the region of a quarter of the critical density: the electron temperature and the magnitude of the characteristic density gradient.

The paper consists of three sections. In §1 we describe the experimental setup and present the main results of the measurement of the spectral composition and intensity of the radiation generated by the plasma near the frequency  $\frac{3}{2}\omega_0$ . In §2 we propose a theory of  $\frac{3}{2}\omega_0$ -harmonic generation in a laser plasma. It is shown that the cause of the appearance of the  $\frac{3}{2}\omega_0$  harmonic is

plasma turbulence, which is triggered by the two-plasmon parametric decay,<sup>[6,12]</sup> the dominant generation process in the region fairly far above the instability threshold being the confluence of three parametrically excited plasma waves of frequencies  $\sim \omega_0/2$ . Section 3 is devoted to the comparison of the theoretical ideas developed with the experimental data and to the discussion of the possibility of using the  $\frac{3}{2}\omega_0$  harmonic for the purpose of plasma diagnostics.

## §1. RESULTS OF THE EXPERIMENTAL INVESTIGATIONS OF THE $\frac{3}{2}\omega_0$ HARMONIC DURING THE IRRADIATION OF MICROSPHERES

For the heating of the plasma we used a nine-channel "Kalmar" neodymium-glass laser setup.<sup>[13]</sup> In contrast to the previous series of experiments,<sup>[14]</sup> in the present work, as in<sup>[15,16]</sup> we used yttrium aluminum garnet as the active element of the master generator. The half-width of the radiation line at the output end of the laser setup was  $\sim 10 \text{ \AA}$  ( $\lambda_0 = 10640 \text{ \AA}$ ), which is significantly less than in the series of experiments.<sup>[14]</sup> The radiation spectrum at the output end of the laser system is shown in Fig. 1. The laser energy in the experiments being described reached 150 J when the light-pulse base width  $\tau \approx 2.5 \text{ nsec}$ , the leading-edge width  $\tau_e \lesssim 0.5 \text{ nsec}$ , and the magnitude of the contrast with respect to energy  $\sim 10^6$ .

The laser radiation from the output end of the amplifier cascades was focused with the aid of nine two-lens systems (of effective focal length  $f = 20 \text{ cm}$ ) on a spherical target located in a vacuum chamber. The degree of linear polarization of the radiation of each beam on the target surface was not high, which was due, in particular, to the depolarization of the radiation in the beam-splitting systems in the stages for power amplification and the guidance of the light beams to the target. All the beams arrived at the target within an interval of time not exceeding  $10^{-10} \text{ sec}$ , which was achieved by equalizing the optical path lengths of the heating beams in the guidance system. Because of Fresnel losses in the guidance system and in the elements of the diagnostic apparatus, the light energy in the target region was  $\sim 100\text{--}120 \text{ J}$ . The focal plane of each of the focusing

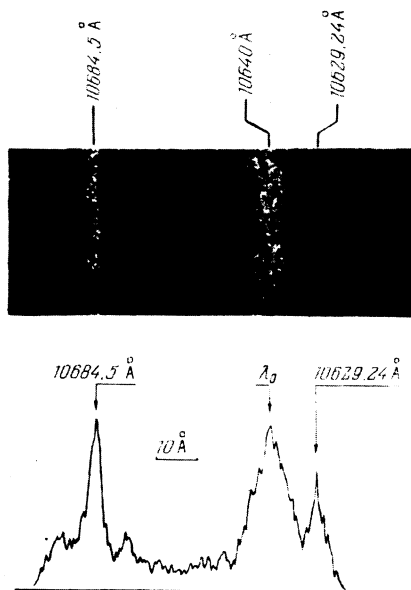


FIG. 1. The spectrogram and microphotogram of the heating radiation at the output end of the laser setup.  $\lambda_0 \approx 10640 \text{ \AA}$ ; the reference lines are 10684.5- and 10629.24-Å lines.

systems was located behind the target, so that the diameter of the light beam in the target plane was  $\sim 150 \mu$ . This allowed us to increase the mean flux density at the target surface, as compared to what obtained earlier,<sup>[15, 16]</sup> to a value  $q \sim 10^{14} \text{ W/cm}^2$ .

As the targets we used solid glass ( $\text{SiO}_2$ ) microspheres of diameters from 70 to 140  $\mu$  and hollow glass microspheres of diameters from 70 to 95  $\mu$  and wall thicknesses from 1.2 to 3.6  $\mu$ . The target was suspended from a rubber-cement fiber whose thickness could have a value of up to 0.5  $\mu$ , and the fiber was fastened to a holder having the shape of a slingshot. The focusing of the radiation on the target in this series remained the same for all the target diameters.

A schematic diagram of the arrangement of the diagnostic apparatus is shown in Fig. 2. The investigation of the  $\frac{3}{2}\omega_0$ -harmonic generation was carried out in two directions, the angle between which was  $\approx 105^\circ$ . In the first direction the image of the target 1 was transmitted to the slit of an MDR-2 diffraction spectrograph with an inverse linear dispersion of 40  $\text{\AA}/\text{mm}$  through one of the focusing systems 2, 3 and the auxiliary lens 5, i.e., the observation was carried out in the backward direction with respect to one of the heating beams in a solid angle  $\approx 3 \times 10^{-2} \text{ sr}$ . In the second direction the image of the target was transmitted with eightfold amplification to the slit of an ISP-51 prism spectrograph having an inverse dispersion  $\approx 136 \text{ \AA}/\text{mm}$  in the  $\frac{3}{2}\omega_0$  region. The transmission of the image was effected through the diagnostic window 7 of the vacuum chamber by means of the long-distance objective 9, whose focal length  $f=300 \text{ mm}$ , and the observation direction coincided with the direction of one of the heating beams. The observation solid angle was  $3.6 \times 10^{-3} \text{ sr}$ .

In both directions we detected the generation of the  $\frac{3}{2}\omega_0$  harmonic with a strongly pronounced doublet struc-

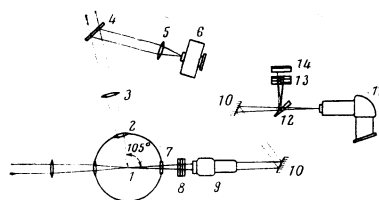


FIG. 2. Schematic diagram of the arrangement of the spectral and diagnostic apparatus: 1) target; 2, 3) one of the focusing systems; 4) plane-parallel plate; 5) lens; 6) MDR-2 spectrograph; 7) diagnostic window; 8) light filters; 9) long-distance objective; 10) mirrors; 11) ISP-51 spectrograph; 12) one-degree wedge; 13) light filters; 14) film holder.

ture. The radiation spectrum near  $\frac{3}{2}\omega_0$  exhibits two components: a red component shifted from the rated value  $\frac{2}{3}\lambda_0 \approx 7093.3 \text{ \AA}$  toward the region of longer wavelengths by an amount that varies from 15 to 32  $\text{\AA}$  and a less intense blue component shifted from the rated value toward the region of shorter wavelengths by an amount that varies from 7 to 13  $\text{\AA}$ . The distance between these two components varied in different flashes from 27 to 42.5  $\text{\AA}$ . The position of the minimum between the peaks corresponded to within 2–3  $\text{\AA}$  to the rated  $\frac{2}{3}\lambda_0$  value. It should be noted that the shifts of the components obtained in simultaneous registrations in the two indicated directions differed from each other: in the majority of flashes, for the spectrograms obtained in the first direction the shift of the red component was less, while the shift of the blue component was greater, than for the spectrograms taken in the second direction. The ratio of the intensity of the blue component to the intensity of the red component varied in different flashes from 0.35 to 0.95. The degree of uniformity of the irradiation of the microspheres was monitored by photographing the plasma in its own x rays by means of pin-hole cameras,<sup>[15, 16]</sup> and was found to be fairly high.

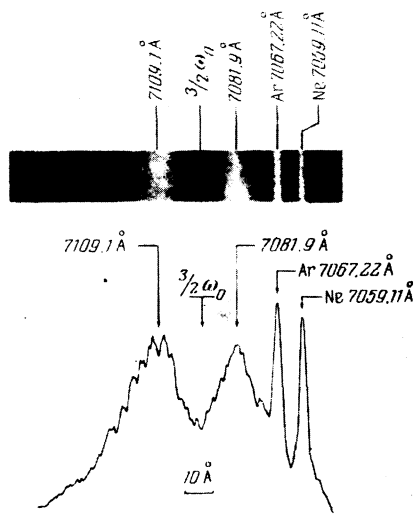


FIG. 3. The spectrogram and microphotogram of the frequency region near  $\frac{3}{2}\omega_0$ , obtained in the first registration direction in the irradiation of a hollow glass microsphere of diameter 83  $\mu$  and wall thickness  $\Delta \sim 3.6 \mu$ . The reference lines are the 7067.22-Å Ar and 7059.11-Å Ne lines.

In Fig. 3 we show the spectrogram and its micro-photogram of the frequency region near  $\frac{3}{2}\omega_0$ , obtained in the first registration direction in the irradiation of a hollow glass microsphere of diameter  $83 \mu$  and wall thickness  $\Delta \approx 3.6 \mu$ . For this spectrogram the width of the red component at the half-intensity level is  $\sim 33 \text{ \AA}$ , while that of the blue component  $\sim 24 \text{ \AA}$ ; the total width of the entire distribution at the level of  $\frac{1}{10}$ -th the maximum intensity is  $\sim 80 \text{ \AA}$ . In virtually all the  $\frac{3}{2}\omega_0$  spectrograms obtained in both observation directions we detected modulation of the spectral distribution of the radiation intensity with the distance between the peaks varying from 3.4 to 11.5  $\text{\AA}$ .

The absolute measurements of the energy of the  $\frac{3}{2}\omega_0$  harmonic that were carried out in the second observation direction showed that the energy emitted into the solid angle of the objective ( $\approx 3.6 \times 10^{-3}$  sr) attains a value of  $10^{-2}$  erg (for a target of diameter  $83 \mu$  and  $\Delta \sim 3.6 \mu$ ). Such an energy value, under the assumption of isotropy of the emission of the harmonic, leads to an estimate of  $3.5 \times 10^{-6}$  J for the energy emitted into the total solid angle of  $4\pi$  sr, and gives a coefficient of conversion into the harmonic of  $\sim 10^{-7}$ . However, the assumption that the  $\frac{3}{2}\omega_0$ -harmonic emission is isotropic requires further experimental verification.

## §2. NONLINEAR CONVERSION OF THE HEATING RADIATION INTO THE $\frac{3}{2}\omega_0$ HARMONIC IN A LASER PLASMA

A fairly complete theoretical study of  $\frac{3}{2}\omega_0$ -harmonic generation in a laser plasma is possible as a result of the fact that it is possible to indicate a limited number of nonlinear processes responsible for this effect. It is now known<sup>[4]</sup> that the generation of the  $\frac{3}{2}\omega_0$  harmonic is connected with the excitation in the laser plasma of parametric instability of the type of decay of the heating light wave of frequency  $\omega_0$  into two electron plasma waves of frequency  $\omega_0/2$  in the region of one-quarter the critical density. The parametric plasma turbulence that then arises leads to the generation of a transverse wave of frequency  $\frac{3}{2}\omega_0$  either as a result of the process of confluence of the incident light wave with a parametrically excited electron plasma oscillation of frequency  $\sim \omega_0/2$ , or as a result of the process of fusion of three plasma waves of frequencies  $\sim \omega_0/2$  into a transverse electromagnetic wave. Below we shall show that, in spite of the fact that the second of the indicated mechanisms is a nonlinear process of a higher order in smallness, it can be the dominant mechanism in a number of practically interesting cases, since the probability of a three-wave process is low as a result of the nonfulfillment of the conditions for resonance with respect to the wavelengths (i. e., of the law of conservation of momentum for three waves participating in a nonlinear interaction).

The analysis of the processes leading to the generation of the  $\frac{3}{2}\omega_0$  harmonic is connected with the solution of the equation of nonlinear interaction of plasma oscillations<sup>[17]</sup>:

$$\frac{\partial}{\partial \omega} [\omega M_{ij}^H(\omega, \mathbf{k})] \frac{\partial}{\partial t} (E_j E_i)_{\omega, \mathbf{k}} - \frac{\partial}{\partial \mathbf{k}} [\omega M_{ij}^H(\omega, \mathbf{k})]$$

$$\begin{aligned} & \times \frac{\partial}{\partial \mathbf{r}} (E_j E_i)_{\omega, \mathbf{k}} = i\omega [e_{ij}(\omega, \mathbf{k}) - e_{ij}^*(\omega, \mathbf{k})] (E_j E_i)_{\omega, \mathbf{k}} \\ & - \frac{1}{2} i\omega A_{ia}^*(\omega, \mathbf{k}) \int d\omega' d\mathbf{k}' (E_r E_c)_{\omega', \mathbf{k}'} (E_j E_b)_{\omega - \omega', \mathbf{k} - \mathbf{k}'} S_{ij}(\omega, \mathbf{k}; \omega', \mathbf{k}') \\ & \times S_{abc}(\omega, \mathbf{k}; \omega', \mathbf{k}') - 6i\omega A_{ia}^*(\omega, \mathbf{k}) \int d\omega' d\mathbf{k}' d\omega'' d\mathbf{k}'' \\ & \times (E_j E_b)_{\omega', \mathbf{k}'} (E_i E_c)_{\omega'', \mathbf{k}''} (E_r E_a)_{\omega - \omega' - \omega'', \mathbf{k} - \mathbf{k}' - \mathbf{k}''} \\ & \times \varepsilon_{ijrs}(\omega, \mathbf{k}; \omega', \mathbf{k}'; \omega'', \mathbf{k}'') \varepsilon_{abcd}(\omega, \mathbf{k}; \omega', \mathbf{k}'; \omega'', \mathbf{k}''). \end{aligned} \quad (1)$$

Here  $M_{ij}^H(\omega, \mathbf{k})$  is the Hermitian part of the Maxwell tensor:

$$M_{ij}(\omega, \mathbf{k}) = \varepsilon_{ij}(\omega, \mathbf{k}) - \frac{c^2 k^2}{\omega^2} \left( \delta_{ij} - \frac{k_i k_j}{k^2} \right),$$

$(E_j E_i)_{\omega, \mathbf{k}}$  is the spectral function of the electric field,  $c$  is the velocity of light,  $\varepsilon_{ij}(\omega, \mathbf{k})$  is the linear-permittivity tensor,  $S_{ijrs}(\omega, \mathbf{k}; \omega', \mathbf{k}')$  and  $\varepsilon_{ijrs}(\omega, \mathbf{k}; \omega', \mathbf{k}'; \omega'', \mathbf{k}'')$  are three- and four-index nonlinear-interaction tensors, explicit expressions for which are given in, for example, <sup>[17]</sup> (see §§7 and 8), and  $A_{ij}(\omega, \mathbf{k}) = M_{ij}^{-1}(\omega, \mathbf{k})$  is the inverse Maxwell tensor. The second and third terms on the right-hand side of Eq. (1) correspond to allowance for the nonlinear interaction in which three and four waves participate and respectively describe in the case of the generation of a transverse wave of frequency  $\omega \approx 3\omega_0/2$  the process of fusion of a transverse wave ( $\omega_0$ ) with a longitudinal plasma wave ( $\omega_0/2$ ) and the fusion of three longitudinal plasma oscillations. The processes in which three waves participate have been fairly well studied (see, for example, the review articles<sup>[17, 18]</sup>). The generation of a transverse wave by the fusion of three longitudinal plasma waves has not been discussed before.

We shall be interested in the steady-state ( $\partial/\partial t = 0$ ) amplitude of the  $\frac{3}{2}\omega_0$  harmonic emitted from the plasma, an amplitude which is established as a result of the competition of three processes: the departure of the excited wave from the region of parametric turbulence (the second term on the left-hand side of (1)), the linear attenuation of the excited transverse wave (the first term on the right-hand side of (1)), and the nonlinear interaction of the waves (the second and third terms on the right-hand side of Eq. (1)). Under the conditions of the laser plasma, the dimension,  $\Delta x$ , of the region of parametric turbulence is small compared to the mean free path of the light wave with respect to electron-ion Coulomb collisions ( $c/\nu_{ei} \gg \Delta x$ ). The first term on the right-hand side of (1) is then small, and the steady state is attained in the case when the departure of the excited waves from the region of parametric turbulence owing to the inhomogeneity of the plasma density is compensated by the generation of transverse waves as a result of the nonlinear processes.

Let us first consider the generation of the  $\frac{3}{2}\omega_0$  harmonic in the fusion of the plasma oscillation with the incident light wave (the process  $l+t-t$ ). Retaining only the second term on the right-hand side of (1) and going over to the spectral densities of the energies of the transverse and longitudinal waves, we obtain in accordance with the formulas (6.64) and (6.65) of the review article<sup>[17]</sup> the equation

$$|\cos \theta| \frac{2\sqrt{2}}{3} c \frac{\partial}{\partial x} W_{3/2}^{lt}(\mathbf{k}) = \frac{e^2 E_0^2 (\mathbf{k} - \mathbf{k}_0)^2}{12m^2 \omega_0^2} \int d\omega \sin^2 \theta' W_l(\mathbf{k} - \mathbf{k}_0) \times \delta(\omega - \omega_l(\mathbf{k} - \mathbf{k}_0) - \omega_0) \varepsilon''(\omega, \mathbf{k}) |\varepsilon(\omega, \mathbf{k}) - c^2 k^2 / \omega^2|^{-2}. \quad (2)$$

Here  $\varepsilon(\omega, \mathbf{k})$  is the transverse permittivity,  $e$  is the electron charge,  $m$  is the electron mass,  $W_l(\mathbf{k} - \mathbf{k}_0)$  is the spectral density of the energy of the longitudinal oscillations with the wave vector  $\mathbf{k} - \mathbf{k}_0$ ,  $\theta$  and  $\theta'$  are the angles between the wave vector  $\mathbf{k}$  of the  $\frac{3}{2}\omega_0$  harmonic and the vector  $\mathbf{k}_0$  ( $k_0 = 3^{1/2}\omega_0/2c$  is the value of the wave number of the pump in the region of a quarter of the critical density) and the intensity vector,  $\mathbf{E}_0$ , of the electromagnetic field of the heating light wave, and  $W_{3/2}^{lt}$  is the spectral density of the energy of the  $\frac{3}{2}\omega_0$  harmonic. The superscript  $lt$  indicates that the harmonic generation is connected with the process of fusion of the incident transverse wave  $l$  with the longitudinal plasma wave  $l$ . The law of dispersion of the parametrically excited plasmons,

$$\omega_l(\mathbf{k}) = \frac{1}{2}\omega_0 [1 + \frac{3}{2} \mathbf{k} \mathbf{k}_0 r_{De}^2]$$

( $r_{De}$  is the electron Debye radius), was obtained earlier<sup>[12]</sup> under the assumption that the wavelength of the excitable plasmons is much shorter than the wavelength of the pump (i. e., that  $k \gg k_0$ ). This assumption is fulfilled in virtually the entire region of parametric turbulence.

During the  $l+t-t$  fusion there is excited in the plasma, in the region of a quarter of the critical density, a transverse wave with the dispersion law  $\frac{3}{2}\omega_0 = (\omega_{Le}^2 + c^2 k_{3/2}^2)^{1/2}$ . The wavelength of the  $\frac{3}{2}\omega_0$  harmonic is comparable to the wavelength of the pump:  $k_{3/2} = (\frac{3}{2})^{1/2} k_0$ . Since the wavelength of the parametrically excitable plasmons is much shorter than the wavelength of the pump ( $k \gg k_0$ ), the law of conservation of momentum,  $\mathbf{k}_{3/2} = \mathbf{k}_0 + \mathbf{k}$ , is not fulfilled and, consequently, the  $l+t-t$  process has a nonresonance character. In Eq. (2) this is manifested in the fact that  $\varepsilon(\omega, k) - (c^2 k^2 / \omega^2) \neq 0$ , as a result of which there arises on the right-hand side of (2) the small factor

$$e'' |\varepsilon - (ck/\omega)^2|^{-2} \sim (\nu_{ei} \omega_0^3 / c^4 k^4) \ll 1.$$

In the above-described experiment the pumping wave was highly depolarized. We shall in the subsequent computations assume the pumping wave to be naturally or circularly polarized. Notice also that the intensity of the  $\frac{3}{2}\omega_0$  harmonic is proportional to the thickness,  $l = \Delta x / |\cos \theta|$ , of the parametrically turbulent plasma layer through which the radiation passes. In a real situation this quantity is always finite, on account of the finiteness of the plasma volume:  $\Delta x < l < l_{\max}$ . During the heating of the microspheres, there occurs a spherically symmetric dispersion of the plasma. Then  $l_{\max} \sim (R \Delta x)^{1/2}$ , where  $R$  is the radius of the sphere on which the plasma density is equal to a quarter of the critical density, and for the energy flux density  $q_{3/2}$  at the frequency  $\frac{3}{2}\omega_0$ :

$$q_{3/2} = \frac{4\sqrt{2}}{3} c \int \frac{dk}{(2\pi)^3} W_{3/2}(\mathbf{k})$$

we obtain from Eq. (2) the equation

$$\frac{\partial}{\partial x} q_{3/2}^{lt} = \left( \frac{\kappa T_e}{mc^2} \right)^2 \frac{\nu_{ei} E_0^2}{k_m^2 r_{De}^2} \frac{E_l^2}{8\pi n_e \kappa T_e} \frac{\ln(R/\Delta x) + 1}{256\pi}. \quad (3)$$

Here  $T_e$  is the electron temperature,  $n_e \approx n_c/4$  is the density,  $n_c = m \omega_0^2 / 4\pi e^2$  is the critical density of the plasma, and  $\kappa$  is the Boltzmann constant. It was assumed in the derivation of Eq. (3) that, in accordance with the results of<sup>[12]</sup>, the spectral energy density,  $W_l(\mathbf{k})$ , of the plasma waves arising as a result of the parametric two-plasmon decay is localized in the form of a narrow (relative to the wavelengths) line near

$$k \approx k_m = r_{De}^{-1} [(\omega_0 - 2\omega_{Le}) / 3\omega_{Le}]^{1/2}$$

( $\omega_{Le}$  is the local Langmuir electron frequency) and is a slowly varying function of the angle between  $\mathbf{k}$  and  $\mathbf{k}_0$ ;  $E_l^2 = \pi^{-2} \int d\mathbf{k} W_l(\mathbf{k})$ .

Notice that Eq. (3) allows us to estimate the parametric-turbulence level  $E_l^2 / 8\pi n_e \kappa T_e$  in terms of the coefficient of conversion of the heating-radiation energy flux  $q = c E_0^2 / 4\pi$  into the  $\frac{3}{2}\omega_0$  harmonic:

$$\frac{q_{3/2}^{lt}}{q} \sim \frac{1}{32} \frac{\nu_{ei} \Delta x}{c k_m^2 r_{De}^2} \left( \frac{\kappa T_e}{mc^2} \right)^2 \frac{E_l^2}{8\pi n_e \kappa T_e}. \quad (4)$$

On the other hand, in<sup>[6,12]</sup> the level of quasi-stationary turbulence in the two-plasmon parametric decay was found:

$$\frac{E_l^2}{8\pi n_e \kappa T_e} = 20p \left( 1 - \frac{1}{p} \right)^2 \frac{\kappa T_e \nu_{ei} \omega_{Le}}{mc^2 \omega_{Le}^2}, \quad (5)$$

where  $p^2 = q/q_{\text{thr}}$  is the excess of the flux  $q$  over the threshold value for the excitation of the two-plasmon parametric decay:

$$q_{\text{thr}} = \frac{32}{3} n_e m c^3 \left( \frac{\nu_{ei}}{\omega_{Le}} \right)^2 \left( 1 + \frac{5\nu_{Te}}{2a\nu_{ei}} \right). \quad (6)$$

Here  $\nu_{Te} = (\kappa T_e / m)^{1/2}$  is the thermal velocity of the electrons,  $a = [d \ln n_e(x) / dx]^{-1}$  is the characteristic dimension of the plasma-density inhomogeneity in the region of a quarter of the critical density.

The formula (6) with allowance for the influence of the plasma inhomogeneity on the threshold for the two-plasmon parametric decay was obtained in<sup>[19]</sup>. For laser-radiation fluxes higher than the threshold value (6), the parametric instability develops in the vicinity of a quarter of the critical density:

$$\frac{n_e}{4} < n_c < \frac{n_c}{4} \left( 1 - \frac{3}{2} \ln^{-1} \frac{\omega_0}{\nu_{ei}} \right). \quad (7)$$

Integrating (3) over the parametric-turbulence region (7), we obtain an expression for the energy-flux density in the  $\frac{3}{2}\omega_0$  harmonic:

$$q_{3/2}^{lt} = 2.3 \cdot 10^{-17} q_{3/2}^{thr} T_e^{3/2} A \frac{a}{\lambda_0} \left( 1 - \frac{1}{p} \right)^2 \left( 1 + 1.4 \cdot 10^6 \frac{\lambda_0^2 T_e^2}{za} \right)^{-1/2}. \quad (8)$$

Here  $q_{3/2}$  and  $q$  are measured in  $\text{W/cm}^2$ ,  $T_e$  in keV,  $a$  and  $\lambda_0 = 2\pi c / \omega_0$  in centimeters;  $A$  and  $z$  are the atomic weight and charge of the ions of the target material.

Notice that the flux density  $q_{3/2}^{lt}$  is proportional to  $q^{3/2}$  and  $T_e^{3/2}$ , the atomic weight, and the inhomogeneity length  $a$ , and is inversely proportional to the wavelength,  $\lambda_0$ , of the pump.

Equation (2) also allows us to find the spectral and angular distributions of the radiation at the frequency  $\frac{3}{2}\omega_0$ . The angular distribution of the harmonic

$$\frac{dq_{3/2}^{lt}}{d \cos \theta} \propto q_{3/2}^{lt} \frac{1 + \cos^2 \theta}{|\cos \theta| + (\Delta x/R)^{1/2}} \quad (9)$$

reveals substantial anisotropy in the emission. The most intense emission of the  $\frac{3}{2}\omega_0$  harmonic occurs at an angle  $\theta \sim \pi/2$  with respect to the heating laser beam. The spectrum of the  $\frac{3}{2}\omega_0$  harmonic, when generated in the  $l+t-t$  fusion process, turns out to be symmetric about the frequency  $\frac{3}{2}\omega_0$ , and consists of two (red and blue) satellites having widths

$$\Delta \omega_{\pm} \approx 2.3 \cdot 10^{-2} \omega_0 T_e^{1/2}, \quad (10)$$

and shifted relative to the value  $\frac{3}{2}\omega_0$  by the amount

$$\delta \omega_{\pm} \approx 4.6 \cdot 10^{-2} T_e \omega_0 |\cos \theta|. \quad (11)$$

Notice that, in contrast to second-harmonic generation,<sup>[3]</sup> the frequency shift (11) does not depend on the energy flux of the heating radiation. A characteristic spectrum of the  $\frac{3}{2}\omega_0$  harmonic is shown in Fig. 4.

Let us now consider the process of fusion of three longitudinal plasma oscillations of frequencies  $\omega_1(\mathbf{k}) \sim \omega_0/2$  into a transverse light wave of frequency  $\frac{3}{2}\omega_0$  (the process  $3l-t$ ). Using the third term in Eq. (1), we can derive for the energy flux density  $q_{3/2}^{3l}$  in a manner similar to the procedure expounded above the following expression:

$$\frac{\partial q_{3/2}^{3l}}{\partial x} = \frac{7\sqrt{2}}{2^2} \pi^2 n_e \kappa T_e \left( \frac{\kappa T_e}{mc^2} \right)^{3/2} \omega_L \kappa_m \tau_{De} \left( \frac{E_L^2}{8\pi n_e \kappa T_e} \right)^3. \quad (12)$$

The  $3l-t$  process, in contrast to the  $l+t-t$ , has a resonance character. Comparing (12) with the corresponding expression (3), we see that  $q_{3/2}^{3l}$  is proportional to the cube of the small turbulence-level value  $E_L^2/8\pi n_e \kappa T_e \ll 1$  for the longitudinal plasma waves. However, the absence in (12) of the small factor  $\nu_{ei}/kc \ll 1$ , which is characteristic of the  $l+t-t$  fusion, leads to a situation in which the  $3l-t$  process may, as shown below, predominate in a number of cases over the  $l+t-t$  process.

Integrating (12) over the parametric-turbulence region, we obtain with the aid of the expression (5) the following expression for the energy-flux density  $q_{3/2}^{3l}$  in the  $\frac{3}{2}\omega_0$  harmonic due to the three-plasmon fusion process:

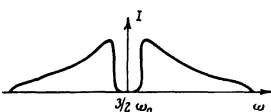


FIG. 4. The spectral composition of the radiation generated by the laser plasma at the frequency  $\frac{3}{2}\omega_0$  in the  $l+t-t$  process.

$$q_{3/2}^{3l} \approx 1.8 \cdot 10^{-15} q_{3/2}^{lt} T_e^{11/2} \left( \frac{A}{z} \right)^3 \frac{a}{\lambda_0} \left( 1 - \frac{1}{p} \right)^6 \left( 1 + 1.4 \cdot 10^6 \frac{\lambda_0^2 T_e^2}{za} \right)^{-1/2}. \quad (13)$$

In contrast to  $q_{3/2}^{lt}$  (see formula (8)),  $q_{3/2}^{3l}$  depends significantly more critically on the plasma temperature ( $\propto T_e^{11/2}$ ) and, in the near-threshold region, on the excess of  $p$  over the threshold ( $\propto (1-1/p)^6$ ). This indicates the possibility that the  $3l-t$  process will be dominant at high plasma temperatures, i. e., at sufficiently high pump fluxes.

The angular distribution

$$dq_{3/2}^{3l}/d \cos \theta \propto q_{3/2}^{3l} [|\cos \theta| + (\Delta x/R)^{1/2}]^{-1}$$

is similar to the distribution  $dq_{3/2}^{lt}/d \cos \theta$  and also has a maximum at angles  $\theta \sim \pi/2$ , but the spectral distributions in these two cases significantly differ from each other. In the  $3l-t$  process the frequency gets shifted relative to the value  $\frac{3}{2}\omega_0$  by the amount

$$\delta \omega_{\pm} \approx 4.8 \cdot 10^{-2} T_e \omega_0 \cos \theta. \quad (14)$$

The sign of the frequency shift (14) occurring in the  $3l-t$  process depends on the angle,  $\theta$ , between the direction of emission of the  $\frac{3}{2}\omega_0$  harmonic and the direction,  $\mathbf{k}_0$ , of the heating light beam. The broadening,  $\Delta \omega_{3/2} \propto \nu_{ei}$ , of the  $\frac{3}{2}\omega_0$  line in the  $3l-t$  process is due primarily to the electron-ion collisions.

It should be noted that the  $3l-t$  process leads to a situation in which the experimentally observed red satellite of the  $\frac{3}{2}\omega_0$  harmonic is more intense than the blue satellite. This is due to the fact that the wave corresponding to the blue satellite propagates from the parametric-turbulence region  $n_e \approx n_c/4$  into the plasma ( $\cos \theta > 0$ ), while the wave corresponding to the red satellite ( $\cos \theta < 0$ ) propagates outwards from the target. Since there exists behind the  $n_e \approx n_c/4$  region in the laser plasma a region,  $n_e \approx \frac{3}{4}n_c$ , which is crucial for the emission at the frequency  $\frac{3}{2}\omega_0$ , the blue satellite reflected from this region will also be detected by the observer. The generation scheme for the blue and red satellites of the  $\frac{3}{2}\omega_0$  harmonic in the  $3l-t$  process is shown in Fig. 5. The absorption of the harmonic near its point of reflection leads to a situation in which the amplitude of the blue satellite is lower by a factor of  $\exp(\frac{2}{3}a'\nu_{ei}/c)$  than the amplitude of the red satellite emitted directly in the direction of the observer. Here  $a'$  is the characteristic dimension of the plasma density inhomogeneity in the region  $n_e \approx \frac{3}{4}n_c$ .

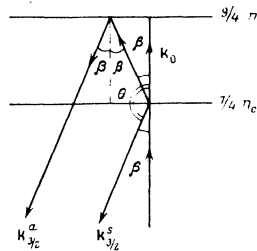


FIG. 5. The generation scheme for the blue and red satellites of the  $\frac{3}{2}\omega_0$  harmonic in the  $3l-t$  process;  $\beta = \pi - \theta$ .

### §3. DISCUSSION OF THE RESULTS

In the present section we show that the above-developed theory enables us to explain the experimentally observed magnitude of the intensity and spectral composition of the radiation emitted near the frequency  $\frac{3}{2}\omega_0$  and to determine on the basis of the experimental data a number of plasma parameters in the region of a quarter of the critical density. The formulas (11) and (14) allow us to relate the observed  $\frac{3}{2}\omega_0$ -harmonic frequency shifts with the plasma temperature in the region of a quarter of the critical density. Since the frequency shifts (11) and (14) virtually coincide, we obtain the following expression for the electron temperature (in keV):

$$T_e \approx \frac{\delta\lambda_n}{\lambda_0} \frac{470}{|\cos\theta|}. \quad (15)$$

For spherically symmetric irradiation, into the formula (15) should be substituted the average value  $|\cos\theta|$ . In our experiment allowance for the irradiation and observation geometries leads to the value  $|\cos\theta| \approx 0.5$ . Choosing as the shift of the satellites of the  $\frac{3}{2}\omega_0$  harmonic relative to the rated value half the experimental (see Fig. 2) distance between the red and blue components,  $\delta\lambda_{3/2} \approx 14 \text{ \AA}$ , we obtain the electron temperature  $T_e \approx 1 \text{ keV}$ . The choice of half the maximum distance between the components as  $\delta\lambda_{3/2}$  is explained by the necessity to exclude the Doppler shift of the spectrum of the  $\frac{3}{2}\omega_0$  harmonic toward the red side by an amount  $\omega_D \sim k_0 v_s$  ( $v_s$  is the speed of sound) because of the motion of the plasma as a whole. For  $T_e \approx 1 \text{ keV}$  the Doppler effect gives a spectrum-shift value  $\sim 5 \text{ \AA}$ , which explains the difference in the measured shifts of the blue,  $\delta\lambda_{3/2}^b \approx 10 \text{ \AA}$ , and red,  $\delta\lambda_{3/2}^r \approx 20 \text{ \AA}$ , components. According to (10), the spectral width of the satellites is  $\sim 100 \text{ \AA}$ , which also agrees with experiment.

The temperature value found with the aid of the expression (15) is roughly two times higher than the value obtainable from x-ray measurements, i. e., the electron temperature in the region  $n_e \approx n_c/4$  is higher than the volume-averaged temperature (determinable from the soft x-ray emission by the method of absorbers). It is convenient to use the relation (15) between the  $\frac{3}{2}\omega_0$ -harmonic shift and the electron temperature in the region of a quarter of the critical density for the purpose of laser-plasma diagnostics.

Let us now proceed to the computation of the intensity  $q_{3/2}$ . For this purpose it is necessary to know the excess, entering into the formulas (8) and (13), of  $p$  over the threshold value. As applied to a laser plasma, it is convenient to write the formula (6) for the two-plasmon parametric instability threshold in the form

$$q_{\text{thr}} = 4.5 \cdot 10^{-3} \frac{z^2}{\lambda_0^4 T_e^3} \left( 1 + 1.4 \cdot 10^6 \frac{\lambda_0^2 T_e^2}{az} \right). \quad (16)$$

Here, as in the formulas (8), (10), (11), and (13)–(15), the flux  $q$  is measured in  $\text{W/cm}^2$ ,  $T_e$  in keV, and  $\lambda_0$  and  $a$  in cm. Thus, all the parameters entering into the expression for the excess,  $p^2 = q/q_{\text{thr}}$ , over the threshold are known except the inhomogeneity dimension. At the above-found temperature of 1 keV, the mean degree of

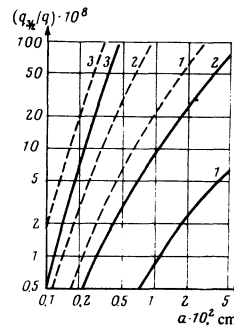


FIG. 6. Plots of the dependence of the conversion coefficient on the inhomogeneity dimension for glass (the solid curves) and polystyrene (the dashed curves). The curves 1 correspond to an electron temperature  $T_e \approx 0.8 \text{ keV}$ , 2)  $T_e \approx 1.0 \text{ keV}$ , 3)  $T_e \approx 1.5 \text{ keV}$ .

ionization of the plasma (a  $\text{SiO}_2$  target) is  $z \approx 9.6$  and the atomic weight  $A \approx 20$ . We use the experimentally obtained coefficient of conversion of the heating light wave into the  $\frac{3}{2}\omega_0$  harmonic to estimate the plasma inhomogeneity dimension in the region of a quarter of the critical density. The  $\frac{3}{2}\omega_0$ -harmonic flux  $q_{3/2} \approx 10^7 \text{ W/cm}^2$  is the total effect of the two processes ( $l+t-t$  and  $3l-t$ ), and into the expression for the energy flux of the  $\frac{3}{2}\omega_0$  harmonic will enter only one parameter to be determined—the inhomogeneity dimension.

In Fig. 6 we show plots constructed from the formulas (8) and (13) with allowance for the expression (16) for different temperature values for glass ( $\text{SiO}_2$ ) and polystyrene ( $\text{C}_8\text{H}_8$ ) targets and exhibiting the connection between the inhomogeneity dimension and the coefficient of conversion into the  $\frac{3}{2}\omega_0$  harmonic. It follows from these plots that the coefficient of conversion increases with increasing inhomogeneity dimension, this dependence becoming more critical with increasing temperature. To the conditions of our experiment corresponds, according to Fig. 6, the value  $a \approx 10^{-2} \text{ cm}$ , the threshold-flux value turning out in this case to be equal to  $q_{\text{thr}} \approx 5 \times 10^{13} \text{ W/cm}^2$ . This enables us to understand why the  $\frac{3}{2}\omega_0$  harmonic was absent under the conditions of the experiments, [15, 16] in which the flux density had a value  $q \sim 10^{13} \text{ W/cm}^2$ . Consequently, the flux  $q \sim 10^{14} \text{ W/cm}^2$  used in the experiment being described exceeds the threshold value by roughly a factor of two ( $p^2 = 2$ ). Then for the above-indicated plasma parameters and excess over the threshold we obtain  $q_{3/2}^{l+t-t} \approx 6 \times 10^{-8} q$ ,  $q_{3/2}^{3l-t} \approx 4 \times 10^{-8} q$ . Thus, under the conditions of our experiment, the two generation mechanisms ( $3l-t$  and  $l+t-t$ ) are equally probable. This means that the amplitudes of the blue and red satellites should differ from each other by a factor of not more than two, the red satellite being more intense than the blue satellite. It is precisely such a situation that was discovered in the experiment (see Fig. 2). As the pump flux is increased, the role of the three-plasmon fusion should significantly increase, owing to the critical dependence of  $q_{3/2}^{3l-t}$  on temperature and the excess over the threshold. If we assume that the dependence  $T_e \propto q^{4/9}$  obtains at flux values  $q \geq 10^{14} \text{ W/cm}^2$ , [7] then, according to (13), the intensity of generation of the  $\frac{3}{2}\omega_0$  harmonic from the laser plasma should increase roughly in proportion to the fourth power of the energy flux density of the pumping wave, i. e., we should have  $q_{3/2} \propto q^4$ . The dependence of  $q_{3/2}$  in the near-threshold generation region,  $q \geq q_{\text{thr}}$ , is determined by the  $l+t-t$  process of fusion of a plasmon with the pumping wave

and has, according to (8), the form  $q_{3/2} \propto (q^{1/2} - q_{\text{thr}}^{1/2})^2 q^{1/2}$ . This dependence can explain the rapid growth, discovered in<sup>[9]</sup>, of the intensity of the  $\frac{3}{2}\omega_0$  harmonic in the near-threshold generation region with increasing pump flux.

The experimentally discovered oscillations in the spectrum of the  $\frac{3}{2}\omega_0$  harmonic can, apparently, be explained by two causes. First, the fine structure of the spectrum may be connected with the irradiation geometry. In the experiment the target was irradiated by nine beams, which, according to (11) and (14), leads to a shift  $\delta\omega_{3/2}$  determined by the direction of each beam with respect to the direction of emission of the harmonic. Therefore, the experimentally observed spikes in the spectral distribution of the radiation intensity may be due to the contributions of the individual laser beams. On the other hand, the oscillations in time of the parametric-turbulence level<sup>[20]</sup> may also be the cause of the modulation of the spectrum of the  $\frac{3}{2}\omega_0$  harmonic.

The dependence, discovered in<sup>[9]</sup>, of the magnitude of the red shift of the  $\frac{3}{2}\omega_0$  harmonic on the target material is apparently connected with the dependence of both the electron temperature and the shape of the surface of the plasma with density equal to a quarter of the critical density on the target material. The effect of the target material on the degree of sphericity of the plasma dispersion, an effect which is characteristic of the case of sharp focusing, can lead to different values of the mean quantity  $|\overline{\cos\theta}|$  for different targets (see the formulas (11) and (14)).

## CONCLUSION

The analysis, performed above by us, of the results of the theory and the experiment allows us to formulate the following proposal for the use of the  $\frac{3}{2}\omega_0$  harmonic for laser-plasma diagnostics. The experimental measurements of the harmonic-frequency shift and the coefficient of conversion of the heating radiation into the  $\frac{3}{2}\omega_0$  harmonic allow us to estimate the electron temperature in the region of a quarter of the critical density (from the formula (15)) and the characteristic scale of variation of the plasma density in the region of a quarter of the critical density (from the known values of  $q$  and  $T_e$ , using (8) and (13)). Thus, the measurement of the intensity and spectral characteristics of the  $\frac{3}{2}\omega_0$  harmonic allows us to find the principal plasma parameters in the region of a quarter of the critical density. A comparison of the quantities  $q_{3/2}^I$  and  $q_{3/2}^II$  (see (8), (13)) then allows us to identify the dominant harmonic-generation mechanism and to estimate from the formulas (4) and (12) the parametric-turbulence level in the region of a quarter of the critical density.

In conclusion, let us note that, besides the above-considered  $\frac{3}{2}\omega_0$ -harmonic generation process, the generation of the third harmonic,  $3\omega_0$ , may also be of interest in connection with laser-plasma diagnostics. The theory developed above is also applicable to this case. The generation of the third harmonic may be the result of a fusion process involving three plasma waves in the critical-density region. The process in which a plasma wave fuses with a second harmonic of the heating radia-

tion will in this case probably be insignificant on account of the smallness of the coefficient of conversion of the pumping radiation into the second harmonic and the nonresonance character of the process. The equation for the flux density of the  $3\omega_0$  harmonic has the same structure as Eq. (12) for the  $\frac{3}{2}\omega_0$ -harmonic generation due to the  $3l-t$  process. For the flux density,  $q_3$ , of the  $3\omega_0$  harmonic in the critical-density region, we obtain the expression

$$q_3 \approx 0.1a\omega_0 n_e \kappa T_e (k_{mrD_e})^3 (\kappa T_e / mc^2)^{1/2} (E_i^2 / 8\pi n_e \kappa T_e)^3.$$

Using for the turbulence level in the critical-density region the results of<sup>[21]</sup>, we obtain the  $3\omega_0$ -harmonic energy flux  $q_3 \approx 10^5$  W/cm<sup>2</sup> for a heating-radiation flux value of  $q \approx 10^{14}$  W/cm<sup>2</sup>.

- <sup>1</sup>N. G. Basov and O. N. Krokhin, Zh. Eksp. Teor. Fiz. **46**, 171 (1964) [Sov. Phys. JETP **19**, 123 (1964)].
- <sup>2</sup>A. A. Rupasov, G. V. Sklizkov, V. P. Tsapenko, and A. S. Shikanov, Zh. Eksp. Teor. Fiz. **65**, 1898 (1973) [Sov. Phys. JETP **38**, 947 (1974)].
- <sup>3</sup>O. N. Krokhin, V. V. Pustovalov, A. A. Rupasov, V. P. Silin, G. V. Sklizkov, A. N. Starodub, V. T. Tikhonchuk, and A. S. Shikanov, Pis'ma Zh. Eksp. Teor. Fiz. **22**, 47 (1975) [JETP Lett. **22**, 21 (1975)].
- <sup>4</sup>N. G. Basov, O. N. Korkhin, V. V. Pustovalov, A. A. Rupasov, V. P. Silin, G. V. Sklizkov, V. T. Tikhonchuk, and A. S. Shikanov, Zh. Eksp. Teor. Fiz. **67**, 118 (1974) [Sov. Phys. JETP **40**, 61 (1975)].
- <sup>5</sup>O. N. Krokhin, Yu. A. Mikhaïlov, V. V. Pustovalov, A. A. Rupasov, V. P. Silin, G. V. Sklizkov, and A. S. Shikanov, Zh. Eksp. Teor. Fiz. **69**, 206 (1975) [Sov. Phys. JETP **42**, 107 (1975)].
- <sup>6</sup>V. Yu. Bychenkov, V. V. Pustovalov, V. P. Silin, and V. T. Tikhonchuk, Fiz. Plazmy **2**, 281 (1976) [Sov. J. Plasma Phys. **2**, 457 (1976)]; Preprint FIAN, No. 45, 1976.
- <sup>7</sup>O. N. Krokhin, G. V. Sklizkov, and A. S. Shikanov, Trudy FIAN SSSR **85**, 143 (1976).
- <sup>8</sup>P. Lee, D. V. Giovanielli, R. P. Godwin, and G. H. McCall, Appl. Phys. Lett. **24**, 406 (1974).
- <sup>9</sup>H. C. Pant, K. Eidmann, P. Sachsenmaier, and R. Sigel, Preprint IPP IV/85, 1975; Opt. Commun. **16**, 396 (1976).
- <sup>10</sup>J. L. Bobin, M. Decroisette, B. Meyer, and Y. Vitel, Phys. Rev. Lett. **30**, 594 (1973); M. Decroisette, B. Meyer, and Y. Vitel, Phys. Lett. **A45**, 443 (1973).
- <sup>11</sup>J. Soares, L. M. Goldman, and M. Lubin, Nucl. Fusion **13**, 829 (1973).
- <sup>12</sup>V. V. Pustovalov, V. P. Silin, and V. T. Tikhonchuk, Zh. Eksp. Teor. Fiz. **65**, 1880 (1973) [Sov. Phys. JETP **38**, 938 (1974)].
- <sup>13</sup>N. G. Basov, O. N. Krokhin, G. V. Sklizkov, S. I. Fedotov, and A. S. Shikanov, Zh. Eksp. Teor. Fiz. **62**, 203 (1972) [Sov. Phys. JETP **35**, 109 (1972)].
- <sup>14</sup>Yu. A. Zakharenkov, N. N. Zorev, O. N. Krokhin, Yu. A. Mikhaïlov, A. A. Rupasov, G. V. Sklizkov, and A. S. Shikanov, Zh. Eksp. Teor. Fiz. **70**, 547 (1976) [Sov. Phys. JETP **43**, No. 2 (1976)].
- <sup>15</sup>N. G. Basov, A. A. Kologrivov, O. N. Krokhin, A. A. Rupasov, G. V. Sklizkov, and A. S. Shikanov, Pis'ma Zh. Eksp. Teor. Fiz. **23**, 474 (1976) [JETP Lett. **23**, 428 (1976)].
- <sup>16</sup>N. G. Basov, Yu. A. Zakharenkov, N. N. Zorev, A. A. Kologrivov, O. N. Krokhin, A. A. Rupasov, G. V. Sklizkov, and A. S. Shikanov, Zh. Eksp. Teor. Fiz. **71**, 1788 (1976) [Sov. Phys. JETP **44**, 938 (1976)].
- <sup>17</sup>V. V. Pustovalov and V. P. Silin, Trudy FIAN **61**, 42 (1972).
- <sup>18</sup>V. N. Tsytovich, Nelineinye éffekty v plazme (Nonlinear Effects in a Plasma), Nauka, 1967 (Eng. Transl., Plenum Pub.

## Variation of the magnetic moment of a charged particle during its nonadiabatic motion in a dipole field

V. D. Il'in and A. N. Il'ina

*Nuclear Physics Institute of the Moscow State University*

(Submitted September 16, 1976)

*Zh. Eksp. Teor. Fiz.* **72**, 983-988 (March 1977)

The law of variation of the magnetic moment of an electron located in a dipole trap and undergoing multiple reflection is investigated. It is shown that for certain initial conditions the measured particle lifetimes agree with the theoretical expression obtained for the change,  $\Delta\mu$ , occurring in the magnetic moment  $\mu$  in one reflection under the assumption that  $\Delta\mu$  is randomly accumulated. An expression is obtained for the coefficient of diffusion due to the nonadiabaticity of the motion.

PACS numbers: 41.70.+t

### INTRODUCTION

The experimental investigation of the nonadiabatic mechanism underlying the losses in magnetic traps is of interest first and foremost from the purely physical point of view, since it is connected with the problem of the appearance of statistical laws in a dynamical system.<sup>[1]</sup> The statistical description arises in the case when the nonlinear oscillations are unstable (i. e., on account of the instability of the dynamical solutions). Analytic semiquantitative estimates for the stochastic instability of the nonlinear electron oscillations in a magnetic trap are given in Chirikov's paper.<sup>[2]</sup> From the standpoint of stochastic theory, the nonadiabatic motion can be presented as statistically irreversible, unstable motion in magnetic-moment space that leads to the diffusion of the particles along the magnetic field. The criteria for such a motion in magnetic fields of different configurations were found earlier,<sup>[3,4]</sup> but the nature of the variation of the invariant (the magnetic moment  $\mu$ ) has itself been little studied. Therefore, the investigation of the law of variation of  $\mu$  during the nonadiabatic motion is important. Furthermore, the nonadiabatic effects are also of great importance from the standpoint of applications to the problem of the dynamics of charged particles in traps of cosmic dimensions, e. g., in the geomagnetic and Jupiter's magnetic traps, whose fields are nearly dipole fields.

The direct determination of the nature of the variation of the adiabatic invariant in multiple reflections through the measurement of the particle lifetimes,  $\bar{\tau}$ , due to the nonadiabaticity does not in itself give any information about the law of variation of  $\mu$ . It is still necessary to prescribe the law of accumulation of  $\Delta\mu$

(the stochastic law, for example), compute the change in  $\mu$  per reflection, and compare the measured mean value of  $\Delta\mu$ , found through  $\bar{\tau}$ , with the theoretical value. The agreement of the theoretical value of  $\Delta\mu$  with the value found with the aid of  $\bar{\tau}$  will in this case be the criterion for the correctness of the chosen law of variation of  $\mu$ .

The present paper is devoted to the investigation of the nature of the variation of the magnetic moment of the electron during the non-adiabatic motion of the electron in a dipole magnetic field.

### MEASUREMENT PROCEDURE AND RESULTS

The experiments were carried out in a dipole trap formed by the field of a uniformly magnetized sphere of diameter 16 cm and magnetic moment  $M = 2.6 \times 10^5$  G cm<sup>2</sup> in a  $\sim 2 \times 10^{-10}$ -Torr ultimate vacuum. The energy of the injected electrons varied from  $\sim 20$  to  $\sim 200$  eV. The injection and registration of the electrons were accomplished in much the same way as were done in<sup>[3]</sup>. The quantity under investigation was the lifetime of the particles in the trap as a function of their energy  $W$ , the angle,  $\alpha$ , between the velocity vector and the line of force, and the distance,  $R_e$ , to the drift shell. The quantity  $R_e$  lies in the median plane  $\theta = \pi/2$  in the spherical coordinate system  $(R, \theta, \varphi)$  with origin on the dipole and axis parallel to the magnetic moment  $\mathbf{M}$ . As the magnitude of the angle  $\alpha$ , we took its value in the median plane ( $\alpha = \alpha(\theta = \pi/2)$ ). The coordinates of the location of the entrance window of the detector in the trap were varied in the range:  $\theta \approx 80 - 50^\circ$ ;  $R_e = 18 - 22$  cm.